

Optical transitions in the two-leg ladder compounds $A_xV_6O_{15}$ ($A = \text{Sr}, \text{Na}$)

V. Ta Phuoc,¹ C. Sellier,² and E. Janod²¹Laboratoire d'électrodynamique des matériaux avancés, CNRS UMR 6157, CEA, Université F.Rabelais, UFR Sciences, Parc de Grandmont, 37200 Tours, France²Institut des Matériaux Jean Rouxel, UMR 6502 CNRS, Université de Nantes, 2, rue de la Houssinière, BP 32229, 44322 Nantes, France

(Received 10 December 2004; published 15 July 2005)

Reflectivity measurements were performed on the quasi-one-dimensional compounds $\text{Sr}_x\text{V}_6\text{O}_{15}$ ($x=0.5, 0.6, 0.7, 0.8, 1.0$) and $\text{NaV}_6\text{O}_{15}$. Two peaks clearly depending on doping are observed in the optical conductivity spectra at 0.8 eV and 1.2 eV. On the basis of recent numerical calculations, these peaks are interpreted in term of local optical transitions within V-O-V rungs forming molecular orbitals, as in α' - NaV_2O_5 . The appearance of two peaks is related to the existence of two different V-O-V rungs, belonging to two different two-legs ladders V1-V3 and V2-V2 in the structure. To explain the doping dependence of these peaks, we propose a scenario in quantitative agreement with experimental results, where V 3d electrons are not spread equally over the different vanadium sites.

DOI: 10.1103/PhysRevB.72.035120

PACS number(s): 78.20.-e, 71.28.+d

I. INTRODUCTION

Due to the interplay between charge, orbital, spin, and lattice degrees of freedom, 3d transition-metal oxides show a large variety of physical properties. As an example, the vanadium bronzes β - $A_xV_6O_{15}$ ($A = \text{Ag}, \text{Na}, \text{Li}, \text{Sr}, \text{Ca}$; the formulation β - $A_{x/3}V_2O_5$ is also used) exhibit remarkable electronic and magnetic properties. These compounds have attracted a lot of attention since a metal-insulator transition (MIT) was observed in $A_{x \approx 1}V_6O_{15}$.^{1,2} Moreover, superconductivity has recently been found under pressure in $\text{NaV}_6\text{O}_{15}$ and $\text{Cu}_{1.19}\text{V}_6\text{O}_{15}$.^{3,4} For the compounds showing a MIT, a charge order takes place in the low-temperature insulating phase.⁵⁻⁸ The origin of the MIT as well as the charge ordering pattern remains an open question. The difference between the magnetic ground state for monovalent $A^+V_6O_{15}$ and divalent cation compounds $A^{2+}V_6O_{15}$ is also a peculiar property which is not understood yet. Indeed, an antiferromagnetic order appears in $A^+V_6O_{15}$ ($A^+ = \text{Ag}^+, \text{Na}^+, \text{Li}^+$),^{2,9} whereas no long-range order exists in $A^{2+}V_6O_{15}$ ($A^{2+} = \text{Ca}^{2+}, \text{Sr}^{2+}$). Moreover, a spin gap has clearly been detected for $\text{SrV}_6\text{O}_{15}$.⁹

$A_xV_6O_{15}$ crystallizes in the space group $C2/m$ for $x \leq 0.9$. The A cations are randomly distributed over the two sites available in the tunnels formed by the V_6O_{15} framework. For $x \geq 0.9$, a zigzag order of the A cations appears inducing a doubling of the unit cell. The structure is then described with the space group $P2_1/a$.^{8,10} Three crystallographically independent vanadium sites V1, V2, and V3 exist in the $C2/m$ structure, as shown in Fig. 1(a). The V1 and V2 vanadium sites are surrounded by an oxygen octahedron, and the V3 site is in a square pyramid environment. Crystallographically, $V1O_6$ and $V3O_5$ polyhedra are arranged in zigzag chains whereas $V2O_6$ octahedra form a ladder along the b axis. However, recent extended Hückel tight-binding (EHTB) calculations have shown that the interchain vanadium-vanadium transfer integrals within the V1 as well as in the V3 zigzag chains are vanishingly small.¹¹ The authors pointed out that an adequate *electronic* description

based on the leading V-V interactions consists of two different nearly orthogonal two-leg ladders running along the b axis—namely, V1-O-V3 and V2-O-V2 ladders—as illustrated in Figs. 1(b) and 1(c).

$A_xV_6O_{15}$ are in a mixed-valence state of V^{4+} ($d^1, S=1/2$) and V^{5+} (d^0), so that the formal valence goes from $V^{4.66+}$ for $\text{SrV}_6\text{O}_{15}$ to $V^{4.83+}$ for $\text{Sr}_{0.5}\text{V}_6\text{O}_{15}$ and $\text{NaV}_6\text{O}_{15}$. Even at room temperature, the valence of the different vanadium sites is unclear. Above the MIT temperature, only one ⁵¹V NMR spectrum is observed for the divalent compounds $\text{Ca}^{2+}V_6O_{15}$ and $\text{Sr}^{2+}V_6O_{15}$,^{2,5} suggesting that the charges are spread over V1, V2, and V3 sites. This is seemingly in contradiction with recent Raman experiments⁷ on $\text{CaV}_6\text{O}_{15}$ suggesting that d electrons occupy only the V1 and V3 sites, the V2 one being empty. On the other hand, early calculations¹² and measurements^{13,14} suggested that electrons occupy mainly V1 sites in monovalent $\text{Na}^+V_6O_{15}$, consistent with recent ⁵¹V NMR experiments indicating the existence of two magnetically different vanadium sites.⁵ Very recently, electron spin resonance (ESR) measurements confirm unambiguously the preferential occupation of d electrons on V1 sites in NaV_6O_{15} .¹⁵

As suggested by the crystallographic structure, the electronic properties are very anisotropic. Transport measurements show a metallic behavior only along the b axis for NaV_6O_{15} ,¹ with an anisotropy ratio $\rho_{\perp b}/\rho_{\parallel b}$ close to 100. Photoemission¹⁶ and optical conductivity⁶ experiments on NaV_6O_{15} suggest a strong electron-phonon coupling, supporting the idea that charge carriers are small polarons.

For the polarization perpendicular to the b axis, optical conductivity spectra exhibit an intense peak at 1 eV in NaV_6O_{15} .¹⁷ The origin of this peak is still unclear and may arise from a local excitation within the V1-O-V3 rung,^{17,18} similarly to the two-leg ladder compound α' - NaV_2O_5 .¹⁹⁻²² In α' - NaV_2O_5 , the two vanadium atoms of a rung are equivalent in the high-temperature phase and have thus the same charge and spin population.²² Precisely, each valence electron is delocalized on a V-O-V rung in such a way that its state can be described by a linear combination of atomic

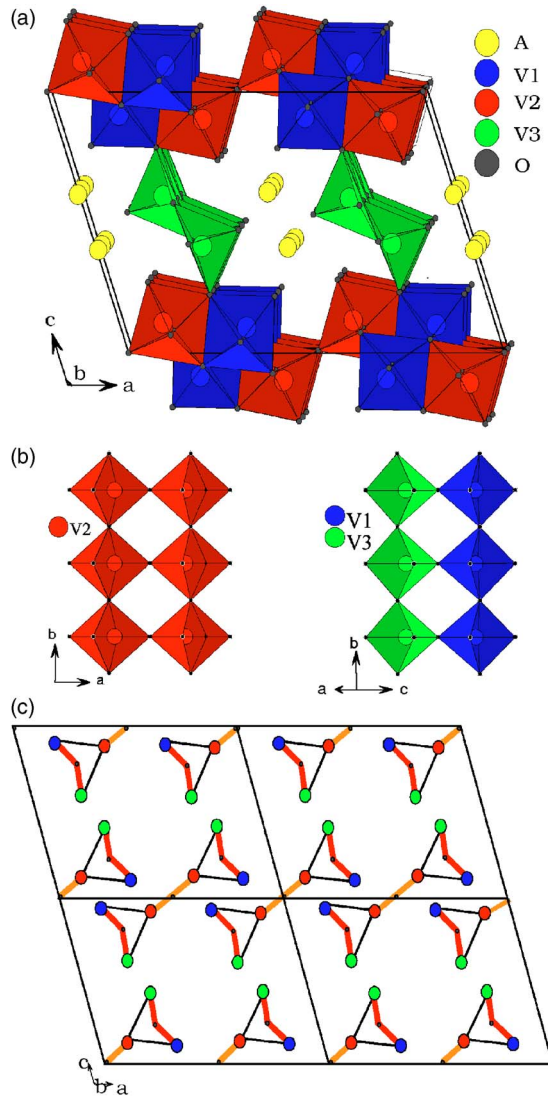


FIG. 1. (Color online) (a) Structure of $A_xV_6O_{15}$ in the $C2/m$ space group, (b) two-leg ladder structure of the V2 (left) and V1-V3 (right) vanadium sites along the b axis, and (c) schematic drawing of the leading V-V transfer integral in the a, c plane as found from EHTB calculations (from Ref. 11). The main interactions (thick lines) are within nearly orthogonal V1-O-V3 and V2-O-V2 rungs. Thin lines denote weaker interactions between the rungs.

orbitals. Thus, the 1-eV peak originates from an on-rung transition between bonding and antibonding orbitals. In $A_xV_6O_{15}$, EHTB calculations also come to the conclusion of the existence of two-leg ladder units along the b axis [two V1-V3 ladders for one V2-V2; see Fig. 1(b)]. Thus, such an optical transition is a good candidate to explain the 1-eV peak in $A_xV_6O_{15}$ compounds. However, a striking difference exists between $A_xV_6O_{15}$ and α' - NaV_2O_5 : the asymmetry of the V-O-V rungs yields an inequivalent charge population for the two vanadium sites within a rung. In NaV_6O_{15} , both V2 and V3 are almost unoccupied.¹⁵ Therefore, the 1-eV optical excitation could arise from a charge transfer from V1 to V3. Note also that, whereas V2-O-V2 rungs are symmetrical for $Sr_xV_6O_{15}$ ($0.5 \leq x \leq 0.9$, $C2/m$ space group), the V2 sites (denoted V2a and V2b) are not equivalent for SrV_6O_{15}

($x=1$, $P2_1/a$ space group).¹¹ Thus, the charge occupancy could be asymmetrical in V2a-O-V2b ladders for SrV_6O_{15} .

In this scenario, as the electronic occupancy of vanadium sites, or equivalently V-O-V rungs, is proportional to x , the 1-eV peak is expected to strongly depend on x in $A_xV_6O_{15}$ compounds.

In this paper, we focus on the dependence of the 1-eV peak seen in optical conductivity with vanadium valence for several divalent cation compounds $Sr_xV_6O_{15}$ ($x=0.5, 0.6, 0.7, 0.8, 1.0$). Furthermore, $Sr_{0.5}V_6O_{15}$ and NaV_6O_{15} , which both have the formal valence 4.83+, are compared. The results suggest that we propose a scenario where the distribution of d electrons over the different vanadium sites and rungs strongly depends on the electronic filling and therefore on the x value. In particular, we argue that only V1-V3 ladders are occupied in $Sr_{0.5}V_6O_{15}$ and NaV_6O_{15} , whereas both V1-V3 and V2-V2 ladders contain d electrons in the spin-gap compound SrV_6O_{15} .

II. EXPERIMENTAL DETAILS

Because no large enough crystals are available for all the compositions, polycrystalline samples were used for this study. The samples of $Sr_xV_6O_{15}$ and NaV_6O_{15} were synthesized by solid-state reactions in silica tubes sealed under vacuum using SrV_2O_6 , $NaVO_3$, V_2O_3 , and V_2O_5 as starting materials. Powder samples of $Sr_xV_6O_{15}$ (NaV_6O_{15}) obtained after a first heat treatment at 650 °C (580 °C) for 33 h were pressed into pellets and heated at the same temperature for 33 h. The starting products SrV_2O_6 ($NaVO_3$) were obtained by heating in air at 600 °C (550 °C) a mixture of $SrCO_3$ (Na_2CO_3) and V_2O_5 . V_2O_3 was synthesized by reduction of V_2O_5 under a H_2 flow at 900 °C for 10 h. Samples were characterized by x-ray diffraction, energy dispersive spectroscopy, and magnetic susceptibility measurements. They were found to be single phased and homogeneous, with a typical dispersion on $x \leq 0.03$. Well-defined signatures of the MIT are observed in the magnetic susceptibility $\chi(T)$ of SrV_6O_{15} and NaV_6O_{15} .

Reflectivity spectra were measured with a BRUKER IFS 66v/S in the range 40–25 000 cm^{-1} from (5 meV to 3 eV). Samples were polished up to optical grade (0.25 μm). After the initial measurement, the samples were coated with a silver film and remeasured. These additional data were used as reference mirrors to calculate the reflectivity in order to take into account light scattering on the surface of the sample. This procedure allows us to *quantitatively* compare the experimental results between the different samples on a large energy range. The optical conductivity spectra were obtained by the Kramers-Krönig (KK) analysis. Prior to the KK transformation, reflectivity spectra were extrapolated above 3 eV using Lorentz oscillators.

III. RESULTS

The optical conductivity for NaV_6O_{15} and $Sr_xV_6O_{15}$ ($x=0.5, 0.6, 0.7, 0.8, 1.0$) is shown in Fig. 2. Surprisingly, the optical conductivity for polycrystalline NaV_6O_{15} is very similar to the spectrum obtained on a single crystal perpen-

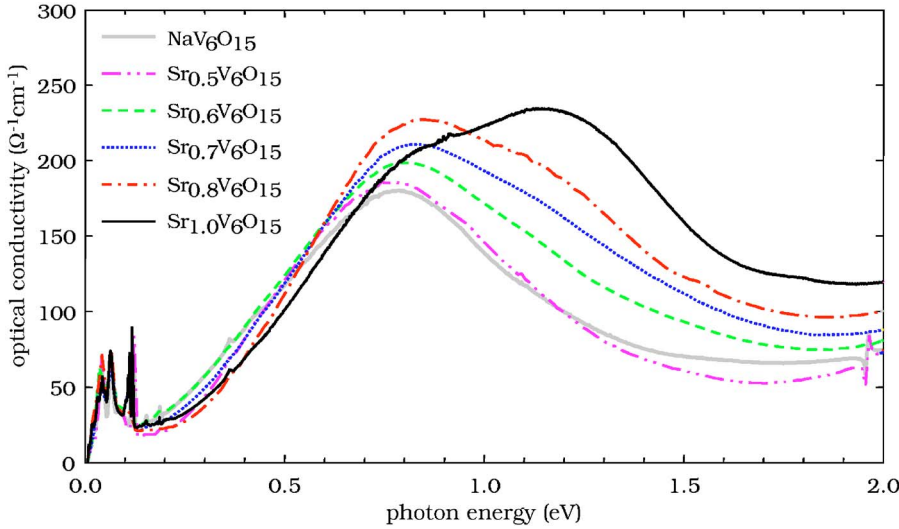


FIG. 2. (Color online) Room-temperature optical conductivity for $\text{Sr}_x\text{V}_6\text{O}_{15}$ ($x=0.5-1.0$) and $\text{NaV}_6\text{O}_{15}$.

dicular to the b axis.¹⁷ Namely, the large peak at 0.37 eV assigned to small polaron hopping along the b axis in a single crystal⁶ is not found. Apart from spiky peaks due to phonons, a flat weak electronic background is observed at low energy. The main midinfrared feature for $\text{NaV}_6\text{O}_{15}$ is a peak located at 0.8 eV which is comparable in frequency and intensity to the peak found on a single crystal perpendicular to the b axis. The slope at high energy is due to a peak above 3 eV, outside the spectral window, usually assigned to $O\ 2p-V\ 3d$ charge transfer.

Although $\text{Sr}_{0.5}\text{V}_6\text{O}_{15}$ and $\text{NaV}_6\text{O}_{15}$ show insulating and metallic behavior along the b axis, respectively, their optical conductivities show remarkable similarities. Indeed, $\text{Sr}_{0.5}\text{V}_6\text{O}_{15}$ exhibits a single midinfrared peak which is comparable in energy and in strength to $\text{NaV}_6\text{O}_{15}$. Note that both compounds share the same formal valence 4.83+ (see Table I) and the same space group $C2/m$ at room temperature. This indicates that the 0.8-eV peak is not related to transport properties (i.e., small polaron hopping). As x increases up to $x=0.8$, the midinfrared spectral weight continuously grows and spectra exhibit a double-peak structure. Indeed, a second peak appears progressively at 1.2 eV without substantial change of the peak at 0.8 eV. For $x=1$, the 0.8-eV peak broadens and slightly shifts to higher energy, and the 1.2-eV peak still grows. Note that although the space group changes from $C2/m$ to $P2_1/a$, the optical conductivity of $\text{SrV}_6\text{O}_{15}$ qualitatively resembles $\text{Sr}_{0.8}\text{V}_6\text{O}_{15}$ and does not show any drastic change or additional feature in the midinfrared range.

TABLE I. Number of d electrons per vanadium site and formal valence.

	d electron/V atom	V formal valence
$\text{NaV}_6\text{O}_{15}$	1/6	+4.8333
$\text{Sr}_{0.5}\text{V}_6\text{O}_{15}$	1/6	+4.8333
$\text{Sr}_{0.6}\text{V}_6\text{O}_{15}$	1/5	+4.80
$\text{Sr}_{0.7}\text{V}_6\text{O}_{15}$	7/30	+4.7667
$\text{Sr}_{0.8}\text{V}_6\text{O}_{15}$	4/15	+4.7333
$\text{Sr}_{1.0}\text{V}_6\text{O}_{15}$	1/3	+4.6667

The optical conductivities of $\text{Sr}_{0.5}\text{V}_6\text{O}_{15}$ and $\text{NaV}_6\text{O}_{15}$ are remarkably similar to the spectra of α' - NaV_2O_5 along the a axis.¹⁹ In α' - NaV_2O_5 , the assignment of the 0.9-eV peak was subject to debate. The 0.9-eV peak was interpreted as an on-site transition between d crystal-field-split levels²³ or as a bonding-antibonding transition between a linear combination of d_{xy} orbitals of two V atoms forming a rung.²⁴ The answer was given by doping-dependent measurements on α' - $\text{Na}_{1-x}\text{Ca}_x\text{V}_2\text{O}_5$ which ruled out the on-site $d-d$ transition. Recently, cluster calculations have confirmed this interpretation and have shown that bridging $O\ 2p$ orbitals with an open-shell character have to be taken into account to describe the initial and final states of this transition.²² As in α' - NaV_2O_5 , the interpretation of the 0.8-eV peak in term of an on-site $d-d$ transition can be ruled out in $\text{A}_x\text{V}_6\text{O}_{15}$. Indeed, such a transition is forbidden by optical selection rules for a free atom. However, this transition could be weakly allowed due to symmetry breaking in the crystal, but its intensity is expected to be very small.

Note that a second peak is also observed at 1.4 eV in α' - NaV_2O_5 and is interpreted as the signature of a “Davidov” splitting due to coupling between adjacent ladders.²⁵ This interpretation can be ruled out for the additional peak observed in $\text{Sr}_x\text{V}_6\text{O}_{15}$ at 1.2 eV. Indeed, if so, this peak would exist in $\text{Sr}_{0.5}\text{V}_6\text{O}_{15}$ and $\text{NaV}_6\text{O}_{15}$, which is not the case. Moreover, in α' - NaV_2O_5 , the 1.4-eV peak is very small compared to the 0.9-eV peak, while in $\text{Sr}_x\text{V}_6\text{O}_{15}$, the intensity of the 1.2-eV peak is of same order as the 0.8-eV peak and strongly depends on x . Thus, the most probable interpretation for both 0.8-eV and 1.2-eV peaks in $\text{A}_x\text{V}_6\text{O}_{15}$ is a transition within different rungs existing in the structure: namely, V1-V3 and V2-V2.

The value of the on-rung effective hopping parameter, obtained from EHTB calculations,¹¹ is larger for V2-V2 ($t_{V2-V2} \approx 0.31$ eV) than for V1-V3 ($t_{V1-V3} \approx 0.22$ eV). This is a key point for our interpretation. Indeed, using the Heitler-London model to describe each single rung as in α' - NaV_2O_5 ,²⁶ one expects two distinct peaks at $\Delta_{V2-V2} \approx 0.65$ eV and $\Delta_{V1-V3} \approx 0.44$ eV in optical conductivity spectra, for V2-V2 and V1-V3 on-rung transitions, respectively. In addition, V1 sites are primarily occupied in $\text{NaV}_6\text{O}_{15}$.¹⁵ Then, only one peak related to a transition from

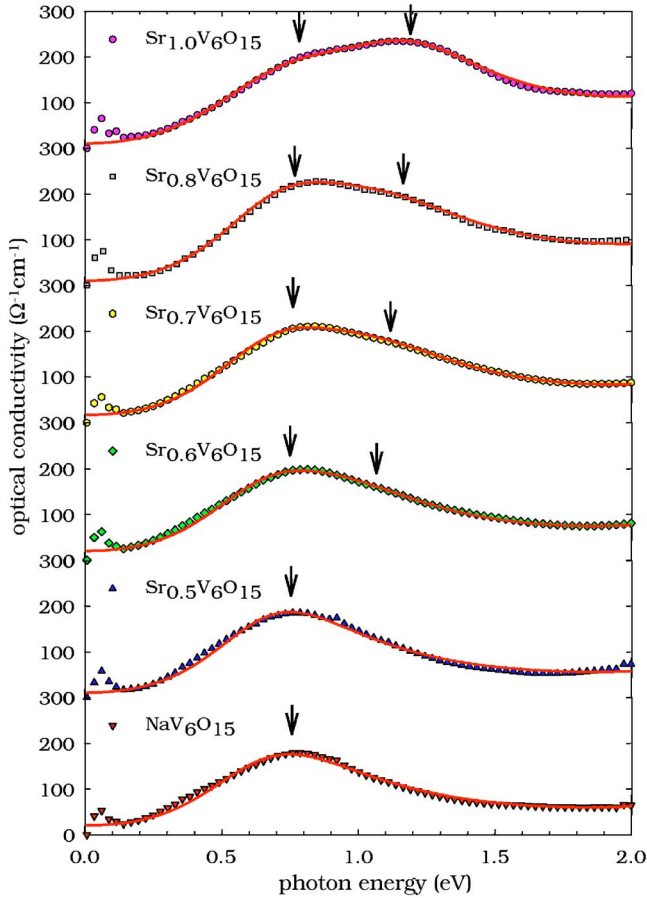


FIG. 3. (Color online) Fit of 0.8-eV and 1.2-eV contributions as described in the text for $\text{Sr}_x\text{V}_6\text{O}_{15}$ ($x=0.5-1.0$) and $\text{NaV}_6\text{O}_{15}$. Symbols are experimental data. Solid lines are a fit. Arrows denote 0.8-eV and 1.2-eV peaks.

V1 to V3 sites is expected in this compound. On the basis of these results, we assign the 0.8-eV and 1.2-eV peaks to transitions within V1-V3 and V2-V2 rungs, respectively. Note that discrepancy between calculated energies and experimental results may arise from the simplicity of the Heitler-London model which does not take into account the $2p$ orbitals of bridging oxygens.

In order to be more quantitative and investigate the occupancy of V1-V3 and V2-V2 rungs as a function of x , we analyzed the optical conductivity in terms of Lorentz oscillators:

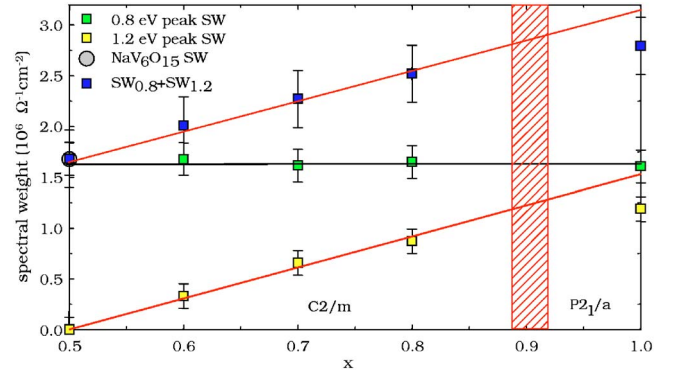


FIG. 4. (Color online) Spectral weight extracted for 0.8-eV and 1.2-eV contributions from the fitting procedure as a function of x . The solid lines are a guide for the eyes. The hatched region denotes the structural $C2/m$ - $P2_1/a$ transition.

$$\sigma(\omega) = \sum_i \frac{S_i \gamma_i \omega^2}{(\omega^2 - \omega_i^2)^2 + \gamma_i^2 \omega^2}, \quad (1)$$

where S_i , γ_i , and ω_i are the strength, damping, and resonance frequency of the i th oscillator, respectively. Three oscillators are used to model the contributions of the 0.8-eV and 1.2-eV peaks and the charge transfer excitation. The results and fit parameters are displayed in Fig. 3 and Table II. This method²⁷ yields to determine separately the spectral weight (SW) of 0.8-eV and 1.2-eV excitations as a function of x , as shown in Fig. 4.

We found that the 0.8-eV peak SW is roughly the same for $\text{NaV}_6\text{O}_{15}$ and $\text{Sr}_{0.5}\text{V}_6\text{O}_{15}$, and remains almost constant as x is increased. In contrast, the SW of the 1.2-eV peak grows linearly with x up to $x \approx 0.8$ from zero to half the SW of the 0.8-eV peak. For $x=1.0$, data diverge from the linear law.

In order to explain the x dependence of both peaks, we propose the following scenario.

(i) For $x=0.5$ and for $\text{NaV}_6\text{O}_{15}$, only one peak is detected at 0.8 eV. Thus, V2-V2 rungs are almost empty and the valence of V2 vanadium is about 5+. Because the structure contains two V1-V3 rungs and one V2-V2 rung, each valence electron is spread over two V1-V3 rungs. According to ESR investigations, the electrons occupy mainly the V1 sites. Therefore, each V1 chain is expected to behave as a quarter-filled chain, as shown in Fig. 5(a).

(ii) For $0.5 < x < 0.8$, the 0.8-eV peak does not change in strength and energy. Thus, there is no signature of a charge

TABLE II. Fit parameters for 0.8-eV and 1.2-eV peaks. Strength is in $\Omega^{-1} \text{eV}^{-2}$, and frequencies and dampings are in eV.

	S_1	γ_1	ω_1	S_2	γ_2	ω_2	S_{CT}	γ_{CT}	ω_{CT}
$\text{NaV}_6\text{O}_{15}$	137.2	0.81	0.75	0	-	-	443.9	0.85	3.2
$\text{Sr}_{0.5}\text{V}_6\text{O}_{15}$	137.1	0.75	0.75	0	-	-	439.6	0.8	3.3
$\text{Sr}_{0.6}\text{V}_6\text{O}_{15}$	137.2	0.81	0.75	26.9	0.75	1.05	457.4	0.85	3.2
$\text{Sr}_{0.7}\text{V}_6\text{O}_{15}$	131.8	0.77	0.76	53.8	0.82	1.14	455.2	0.85	3.2
$\text{Sr}_{0.8}\text{V}_6\text{O}_{15}$	134.6	0.75	0.77	71.3	0.84	1.16	448.3	0.85	3.2
$\text{Sr}_{1.0}\text{V}_6\text{O}_{15}$	132.3	0.88	0.79	96.9	0.74	1.22	453.9	0.8	3.1

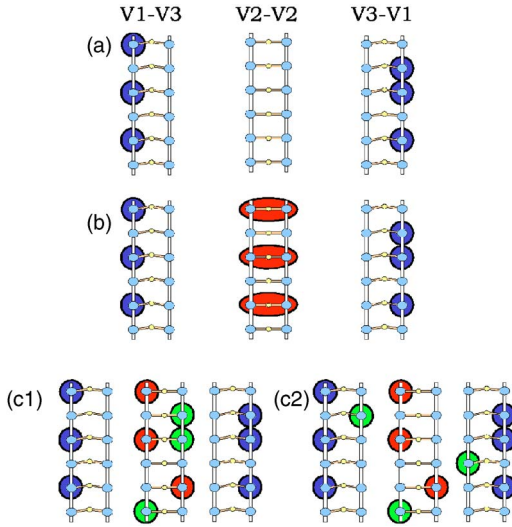


FIG. 5. (Color online) Scenario of the filling of V1-V3 and V2-V2 rungs as a function of x . Dark circles (ellipses) denote sites (rungs) occupied with one d electron. (a) For $x=0.5$, according to ESR experiment (Ref. 15), d electrons mainly occupy V1 sites, and only the half of V1 sites are filled. V2-V2 rungs are unoccupied. (b) For $0.5 < x < 0.8$, the V2-V2 rungs are progressively occupied. No substantial charge redistribution occurs in V1-V3 rungs. (c) For $x > 0.8$, a charge dismutation may occur in the V2-O-V2 rungs due to the $C2/m \rightarrow P2_1/a$ structural transition. Additional electrons can fill empty or singly occupied V2-V2 rungs (c1) or be redistributed over both V2-V2 and V1-V3 rungs (c2).

redistribution within V1-V3 rungs as x is increased. Simultaneously, the 1.2-eV peak increases, indicating that V2-V2 rungs are gradually filled. Note that for $x=0.75$, the SW of the 1.2-eV peak is twice smaller than the SW of the 0.8-eV peak. This is in agreement with the ratio 1:2 between V2-V2 and V1-V3 rungs and *quantitatively* supports our interpretation. From symmetry arguments, no charge dismutation is expected within the V2-O-V2 rungs. The V2-V2 ladders are therefore equivalent to a quarter-filled chain for $x=0.75$, considering each rung as a single site [see Fig. 5(b)].

(iii) For $x=1$, the 1.2-eV peak still increases, but the mid-infrared SW seems to slightly diverge from the linear law. Indeed, one expects that the whole SW for $x=1.0$ is twice the SW for $x=0.5$, because the average V site occupancy is $1/3$ and $1/6$, respectively. This coincides with the structural transition from $C2/m$ to $P2_1/a$ and the existence of a MIT. This SW loss remains unclear at this stage. If the additional electrons between $x=0.8$ and $x=1$ came in both V2a and V2b sites of the V2-V2 ladder, $\text{SrV}_6\text{O}_{15}$ would be described as two quarter-filled V1 chains plus a quarter-filled V2-V2 ladder (one electron per V2-V2 rung, as in α' - NaV_2O_5). An electronic transfer from the electron-rich V2-V2 ladder to the electron-poor V3 site one is also plausible to minimize the repulsive Coulomb interactions, as depicted in Fig. 5(c2). Alternatively, a charge redistribution between singly and doubly occupied V2-V2 rungs could explain the SW loss, as seen in electron-doped α' - $\text{Na}_{1-x}\text{Ca}_x\text{V}_2\text{O}_5$.²⁵ However, the energetic cost due to Coulomb interaction would be unfavorable in this situation.

The scenario is displayed in Fig. 5. Note that it provides a natural explanation to the maximum intensity observed at

$k \sim \pm \pi/4b$ in recent angle-resolved photoemission experiments on $\text{NaV}_6\text{O}_{15}$.¹⁶ Such a maximum is indeed expected for the quarter-filled V1 chain proposed in our scenario.^{16,28} It is also compatible with room-temperature NMR experiments, since two NMR spectra are observed in monovalent $\text{NaV}_6\text{O}_{15}$, while only one spectrum is found for divalent $\text{CaV}_6\text{O}_{15}$ and $\text{SrV}_6\text{O}_{15}$.^{2,5} It could be related to the existence of unoccupied V2 and partly occupied V1 sites for $\text{NaV}_6\text{O}_{15}$ and $\text{Sr}_{0.5}\text{V}_6\text{O}_{15}$, and both sites partly occupied for $\text{SrV}_6\text{O}_{15}$ and $\text{CaV}_6\text{O}_{15}$. Finally, this scenario is also consistent with very recent ESR measurements on $\text{NaV}_6\text{O}_{15}$ which show that electrons are mainly located on V1 sites, and V2 sites are almost unoccupied.¹⁵ Note that this scenario gives some clue to understand the striking similarity of the structural transition associated with the MIT in $\text{NaV}_6\text{O}_{15}$ and $\text{SrV}_6\text{O}_{15}$ (threefold increase of unit cell along the b axis), despite a very different electronic filling. The filling of the V1-V3 ladder could indeed be essentially identical between $\text{NaV}_6\text{O}_{15}$ [Fig. 5(a)] and $\text{SrV}_6\text{O}_{15}$ [see, e.g., Fig. 5(c1)], suggesting a similar charge order pattern in the V1-V3 subunit in both compounds. It also suggests that the mechanism of the metal-insulator transition in $\text{NaV}_6\text{O}_{15}$ and $\text{SrV}_6\text{O}_{15}$ is related to the V1-V3 rather than to the V2-V2 ladder. Note also that the Na (Sr) ordering seems to be required for the MIT to occur. Indeed, although the electronic filling is expected to be similar in $\text{NaV}_6\text{O}_{15}$ and $\text{Sr}_{0.5}\text{V}_6\text{O}_{15}$, $\text{Sr}_{0.5}\text{V}_6\text{O}_{15}$ compounds do not exhibit a MIT. Moreover, the one-dimensional (1D) electronic confinement proposed in this scenario for $\text{NaV}_6\text{O}_{15}$ suggests a close similarity between this compound and the prototypical 1D organic conductor $(\text{TMTSF})_2\text{PF}_6$. Both are strongly correlated quasi-1D systems near quarter filling with a long-range-ordered antiferromagnetic ground state at ambient pressure and showing superconductivity under pressure.^{3,29} This may point to a common origin of the superconductivity in both families, possibly nonconventional.²⁹

The cluster model accurately predicts the energy of the 1-eV peak and the charge and spin balance within a rung in α' - NaV_2O_5 .²² Hence, further *ab initio* cluster calculations are required to clarify the physical origin of the 0.8-eV and 1.2-eV peaks in $A_x\text{V}_6\text{O}_{15}$ compounds. In particular, calculations would be useful to determine the charge distribution of V1/V3 sites and within V2-V2 rungs as a function of x . On the other hand, x -dependent ESR experiments on $\text{SrV}_6\text{O}_{15}$ could probe the occupancy of V2 sites.

IV. CONCLUSION

Reflectivity measurements for $\text{Sr}_x\text{V}_6\text{O}_{15}$ and $\text{NaV}_6\text{O}_{15}$ were performed at room temperature for x ranging from 0.5 to 1.0. Optical conductivity spectra clearly show two mid-infrared peaks depending on x . On the basis of recent EHTB calculations, these excitations have been interpreted as transitions within two different kind of rungs—namely, V1-O-V3 and V2-O-V2—existing in the structure. Following this assignment, we proposed a rung-ladder filling scenario, in quantitative agreement with experiments, to describe the x dependence of the optical conductivity. This scenario could also be consistent with NMR studies showing a difference

between monovalent and divalent compounds even at room temperature, and recent angle-resolved photoemission spectroscopy and ESR experiments on $\text{NaV}_6\text{O}_{15}$. It also provides a valuable starting point to elucidate the charge order pattern arising below the metal-insulator transition in $\text{NaV}_6\text{O}_{15}$ and $\text{SrV}_6\text{O}_{15}$. Temperature- and polarization-dependent optical measurements are clearly needed in this context. Finally, as

for α' - $\text{NaV}_2\text{O}_{15}$, *ab initio* cluster calculations could ultimately confirm the assignment of the midinfrared peaks.

ACKNOWLEDGMENT

The authors thank F. Boucher, M.-L. Doublet, and M.-B. Lepetit for helpful discussions.

-
- ¹H. Yamada and Y. Ueda, J. Phys. Soc. Jpn. **68**, 2735 (1999).
²Y. Ueda, J. Phys. Soc. Jpn. **69**, Suppl. B, 149 (2000).
³T. Yamauchi, Y. Ueda, and N. Mori, Phys. Rev. Lett. **89**, 057002 (2002).
⁴Y. Ueda, M. Isobe, and T. Yamauchi, J. Phys. Chem. Solids **63**, 951 (2002).
⁵M. Itoh, N. Akimoto, H. Yamada, M. Isobe, and Y. Ueda, J. Phys. Chem. Solids **62**, 351 (2001).
⁶C. Presura, M. Popinciuc, P. H. M. van Loosdrecht, D. van der Marel, M. Mostovoy, T. Yamauchi, and Y. Ueda, Phys. Rev. Lett. **90**, 026402 (2003).
⁷Z. V. Popovic, M. J. Konstantinovic, V. V. Moshchalkov, M. Isobe, and Y. Ueda, J. Phys.: Condens. Matter **15**, L139 (2003).
⁸C. Sellier, F. Boucher, and E. Janod, Solid State Sci. **5**, 591 (2003).
⁹Y. Ueda, H. Yamada, M. Isobe, and T. Yamauchi, J. Alloys Compd. **317-318**, 109 (2001).
¹⁰J.-I. Yamaura, M. Isobe, H. Yamada, T. Yamauchi, and Y. Ueda, J. Phys. Chem. Solids **63**, 957 (2002).
¹¹M.-L. Doublet and M.-B. Lepetit, Phys. Rev. B **71**, 075119 (2005).
¹²J. B. Goodenough, J. Solid State Chem. **1**, 349 (1970).
¹³T. Erata, T. Takahashi, and H. Nagasawa, Solid State Commun. **39**, 321 (1981).
¹⁴H. Nagasawa, T. Takahashi, T. Erata, M. Onoda, Y. Kanai, and S. Kagoshima, Mol. Cryst. Liq. Cryst. **86**, 195 (1982).
¹⁵M. Heinrich, H.-A. Krug von Nidda, R. M. Eremina, A. Loidl, Ch. Helbig, G. Obermeier, and S. Horn, Phys. Rev. Lett. **93**, 116402 (2004).
¹⁶K. Okazaki, A. Fujimori, T. Yamauchi, and Y. Ueda, Phys. Rev. B **69**, 140506(R) (2004).
¹⁷P. H. M. van Loosdrecht, C. Presura, M. Popinciuc, M. Mostovoy, G. Maris, T. T. M. Palstra, P. J. M. van Bentum, H. Yamada, T. Yamauchi, and Y. Ueda, J. Supercond. **15**, 587 (2002).
¹⁸C. Presura, Ph.D thesis, University of Groningen, 2003.
¹⁹A. Damascelli, C. Presura, D. van der Marel, J. Jegoudez, and A. Revcolevschi, Phys. Rev. B **61**, 2535 (2000).
²⁰W. S. Bacsa, R. Lewandowska, A. Zwick, and P. Millet, Phys. Rev. B **61**, R14885 (2000).
²¹M. J. Konstantinovic, Z. V. Popovic, V. V. Moshchalkov, C. Presura, R. Gajic, M. Isobe, and Y. Ueda, Phys. Rev. B **65**, 245103 (2002).
²²N. Suaud and M. B. Lepetit, Phys. Rev. Lett. **88**, 056405 (2002).
²³S. A. Golubchik, M. Isobe, A. N. Ivlev, B. N. Mavrin, M. N. Popova, A. B. Sushkov, Y. Ueda, and A. N. Vasil'ev, J. Phys. Soc. Jpn. **66**, 4042 (1997).
²⁴A. Damascelli, D. van der Marel, M. Grüninger, C. Presura, T. T. M. Palstra, J. Jegoudez, and A. Revcolevschi, Phys. Rev. Lett. **81**, 918 (1998).
²⁵C. Presura, D. van der Marel, M. Dischner, C. Geibel, and R. K. Kremer, Phys. Rev. B **62**, 16522 (2000).
²⁶P. Horsch and F. Mack, Eur. Phys. J. B **5**, 367 (1998).
²⁷Different sets of parameters were considered to improve the reliability of the fit procedure, but yielded to equivalent results. In particular, the error bars for the spectral weight were obtained by using these different set of parameters for the SW calculation.
²⁸In the present scenario, the V1 chain in $\text{NaV}_6\text{O}_{15}$ is effectively quarter filled only above 220–240 K. Below this temperature, the dimerization along the *b* axis due to Na ordering leads to an effective description in terms of the half-filled chain.
²⁹D. Jérôme, J. Phys. IV **10**, Pr3, 69 (2000).